Complexation of Lipofectamine and Cholesterol-Modified DNA Sequences Studied by Single-Molecule Fluorescence Techniques

Anca Margineanu,[†] Steven De Feyter,[†] Sergey Melnikov,[†,§] Damien Marchand,[‡] Arthur van Aerschot,[‡] Piet Herdewijn,[‡] Satoshi Habuchi,[†,||] Frans C. De Schryver,[†] and Johan Hofkens*[,†]

Laboratory of Photochemistry and Spectroscopy, Catholic University of Leuven, Celestijnenlaan 200F, B-3000 Leuven, Belgium, and Laboratory for Medicinal Chemistry, Rega Institute, Catholic University of Leuven, Minderbroedersstraat 10, B-3000 Leuven, Belgium

Received May 3, 2007; Revised Manuscript Received August 10, 2007

Lipoplex formation for normal and cholesterol-modified oligonucleotides is investigated by fluorescence correlation spectroscopy (FCS). To overcome the problems related to the fitting of autocorrelation curves when fluorescence bursts are present, the baseline fluorescence levels and the fluorescence bursts in the same trace were separately analyzed. This approach was not previously used in FCS studies of lipoplexes and allowed a more detailed characterization of this heterogeneous system. From the baseline levels, the number of free/bound DNA molecules and the presence of tens to hundreds of nanometer-sized lipoplexes were estimated using various mathematical models. Analysis of the fluorescent bursts provided an indication about the sizes of the lipoplexes, the number of DNA molecules in these aggregates, and the relative amount of lipids in each aggregate. An explanation for the higher transfection efficiency previously reported for one of the cholesterol-modified oligonucleotide compounds was found in relation to the formation of large size lipoplexes.

Introduction

Numerous studies are presently performed to improve gene delivery systems such as cationic liposomes, cationic polymers, amphiphilic α-helical proteins with cationic amino acids, or nanoparticles in view of their possible applications for gene therapy (in tumors, cystic fibrosis, or myopathies) or to manipulate the protein synthesis of cells in culture (e.g., to label proteins of interest using autofluorescent proteins such as the green fluorescent protein). These systems are preferred over the viral vectors (with quite high transfection ability) because the retroviruses used in vivo can cause mutagenesis and tumor induction, as well as various immunological responses, besides their lack of cell-specific targeting.[1−4]

Lipoplexes are complexes formed between DNA and cationic lipids (liposomes or micelles), while those formed between DNA and cationic polymers are known as polyplexes. Even though their formation is simply driven by electrostatic forces, controlling the size and structure of lipoplexes (which are relevant for the transfection efficiency) has proven to be a very complicated process. Multiple factors can influence lipoplex formation, such as the ratio between the number of negative charges in DNA over the number of positive charges of the lipids, the fluidity of the lipid bilayer and the formation of lipid domains after DNA binding, and the presence of cholesterol and of phospholipids triggering the formation of the inverted hexagonal phase.[3,5]

Understanding the structural characteristics on the one hand and the kinetics and thermodynamics of lipoplex formation on the other hand requires the use of complementary techniques (for a review, see ref 6). The structure and the size of DNA−cationic lipid complexes can be investigated by cryo-transmission electron microscopy and X-ray diffraction.[7,8] According to these studies, lipoplexes have a multilamellar structure with repeat distances equivalent to the thickness of a lipid bilayer and a single DNA double helix. Hexagonal arrays were also observed.[9] Alternatively, their size distribution can be evaluated by static/dynamic light scattering,[10,11] by atomic force microscopy,[12] or by light microscopy when complexes are above the resolution of the optical microscope (∼0.3 μm).[13] All of these results point to a very high heterogeneity of the lipoplex size, ranging from 100 or 200 nm up to 1−2 μm.

On the other hand, information about the dynamics of the molecular associations in lipoplexes and the quantification of free and bound DNA can be obtained by fluorescence resonance energy transfer (FRET) between fluorescent probe labeled lipid vesicles/micelles and chromophores attached (covalently or not) to DNA.[14,15] FRET can take place over distances of a few nanometers, meaning that only the DNA bound to the surface of liposomes will contribute to the variation of the measured signal. This eliminates the need to separate the free and the bound fractions. The degree of DNA complexation can also be quantified by ethidium bromide accessibility[16] or by DNA labeling after separation of complexes by gel electrophoresis or ultracentrifugation.[17,18] However, for these two methods, the interpretation of results should be done with caution. For example, ethidium bromide intercalation was demonstrated to be more sensitive to the degree of DNA condensation and not

* Author to whom correspondence should be addressed. Phone: +3216327804. Fax: +3216327990. E-mail: Johan.Hofkens@chem.kuleuven.be.

[†] Laboratory of Photochemistry and Spectroscopy.

[‡] Laboratory for Medicinal Chemistry, Rega Institute.

[§] Present address: Max Planck Institute for Dynamics of Complex Technical Systems, Sandtorstrasse 1, 39106 Magdeburg, Germany.

[||] Present address: Department of Biological Chemistry and Molecular Pharmacology, Harvard Medical School, 250 Longwood Avenue, Boston, MA 02115.

10.1021/bm700486q CCC: $37.00
Published on Web 10/25/2007

to DNA association with lipids,[6,16] while the separation of complexes by electrophoresis or centrifugation was shown to induce further aggregation.[11]

Recently, single-molecule (SM) techniques such as fluorescence correlation spectroscopy (FCS) have been applied to investigate the interaction between DNA and cationic lipids[19−24] or polymers[25−27] as well as the delivery of these systems in living cells.[28,29] There are several advantages when SM techniques are used. First, the ensemble methods can offer only average information about the properties of these complexes. On the contrary, SM techniques are particularly suitable to obtain information about highly heterogeneous systems such as lipoplexes because they allow the study of each individual particle. In SM experiments, histograms for statistically relevant numbers of molecules/particles are constructed to characterize the behavior of the entire population. Second, as we will show in this article, information about lipoplex size and quantification of free and bound DNA can be simultaneously obtained in the same experiment by applying SM techniques. This is in contrast with ensemble measurements, where complementary techniques should be used (e.g., dynamic light scattering to evaluate the complex sizes and FRET for the degree of DNA complexation). Third, SM experiments can offer information that cannot be extracted from ensemble measurements (e.g., the number of molecules in each complex).

In FCS, data about diffusion and complexation kinetics are extracted from the fluorescence intensity fluctuations originating from the varying number of particles in the laser focus.[30−32] When dealing with molecular association between the DNA and the cationic lipids, the formation of very large particles can occur, leading to the appearance of bursts (or spikes) in the fluorescence trace. The presence of these spikes was recognized to alter the shape of the autocorrelation curve, which cannot be fitted with routine mathematical models.[25,33,34] Other methods for the analysis of fluorescence intensity fluctuations, such as high-order autocorrelation functions,[35,36] analysis of fluctuation moments,[37] photon counting histogram, (PCHs),[38] or fluorescence intensity distribution analysis (FIDA)[39] are also not applicable when rare but bright spikes are present.[33] To make the analysis possible for this type of measurements, a statistical method was developed by Van Craenenbroeck et al.[33] from which the amount of bound ligand can be determined. Alternatively, authors are either constructing autocorrelation curves for samples showing only constant fluorescent levels and no fluorescence bursts, or they are only analyzing the count distribution when bright fluorescent spikes are present.[20,24,25] The autocorrelation functions built for traces showing fluorescence bursts could be analyzed only in the case when their shape is not disturbed.[21]

In our approach, we separate for each individual trace the baseline fluorescence level and the fluorescent bursts, and a different analysis is carried out. For the constant levels between bursts, the temporal fluorescence intensity fluctuations (autocorrelation curves) and the amplitudes of the fluorescence intensity fluctuations (high-order autocorrelation functions) give information about the diffusion coefficients and the number of free ligands as well as about the size of the nanometer-scale complexes. The histograms of fluorescence bursts offer statistics about the micrometer-scale lipoplexes. Finally, calculation of the amount of bound and free ligand is possible. In this way, a more detailed characterization of the highly heterogeneous system represented by lipoplexes is feasible. This analysis was possible by using a commercially available PC card for time correlated single photon counting (TCSPC) developed for single-molecule experiments (SPC-630, Becker & Hickl Gmbh, Germany). Data are stored with a time resolution of 50 ns, so they can be imported (e.g., Labview, Matlab, or home-made programs) and rebinned on any time scale necessary for the different mathematical approaches. The advantages of this acquisition mode over the classical hardware autocorrelator have been discussed by other groups as well.[40]

The data acquisition and analysis explained above are applied to study the complexation (i.e., to quantify the amount of free and bound DNA) of double-stranded oligonucleotides with the commercially available cationic lipid Lipofectamine (Invitrogen). The final purpose of the experiment is the intracellular delivery of the antisense oligonucleotide specific for the *MDR1* gene encoding the P-glycoprotein to block the synthesis of this membrane transporter responsible for the resistance of neoplasic cells to chemotherapy.[41] The antisense oligonucleotide is fluorescently labeled and is hybridized with complementary sequences. Besides the normal complementary sequence, two types of cholesterol-modified oligonucleotides were used. One contains a single complementary oligonucleotide linked to cholesterol, and the other one contains four complementary oligonucleotides attached to a cholesterol molecule. This strategy for the intracellular delivery of the antisense *MDR1* sequence was chosen for several reasons. On the one hand, it was already shown that increased transfection efficiency of oligonucleotides is obtained when double-stranded DNA is used instead of single-stranded forms.[42] On the other hand, cholesterol-modified oligonucleotides were demonstrated to have an increased cellular association and improved transfection efficiency.[43] In addition, their delivery into cells can be obtained by using less toxic particles (e.g., low-density lipoproteins), because cholesterol is able to partition into the lipid fraction, thus avoiding the use of cationic phospholipids.[43] The use of double-stranded cholesterol-modified oligonucleotides was tested as a possibility to improve the transfection efficiency.[44] In this case, the cholesterol-modified sequence has only the role to transport the antisense oligonucleotide, and even if it is temporarily trapped in endosomes (due to the possible association of cholesterol with their membranes), the antisense sequence can be released and further diffuse into the nucleus.

Materials and Methods

DNA Sequences. The tetramethyl rhodamine (TMR)-labeled 20 oligonucleotide antisense sequence corresponding to the gene encoding the P-glycoprotein[45] (Figure 1) was obtained from Invitrogen and was hybridized with a complementary 18 oligonucleotide sequence (Invitrogen). Hybridization of 1 nM TMR-labeled oligonucleotide and 1 nM complementary oligonucleotide was performed in a final volume of 30 μL of phosphate-buffered saline (PBS) pH = 7.4 (Sigma) by heating the samples at 80 °C for 3 min, followed by cooling down at room temperature for 15 min.[42]

The DNA concentration was estimated by measuring the optical density of the solutions at 260 nm with a Perkin-Elmer Lambda 40 spectrophotometer (Wellesley, MA), using the extinction coefficient values reported in the literature.[46]

The synthesis of the cholesterol-modified antisense 18 oligonucleotide strands was published elsewhere.[44] In one derivative, the 18 sequence was attached through a polylysine spacer to one cholesterol molecule (1DNA−Ch), and in a second one, four oligonucleotide strands were attached to one cholesterol molecule (4DNA−Ch) (Figure 1).

The cholesterol-modified sequences were hybridized with the TMR-labeled 20 oligonucleotide antisense sequence following the procedure described above.

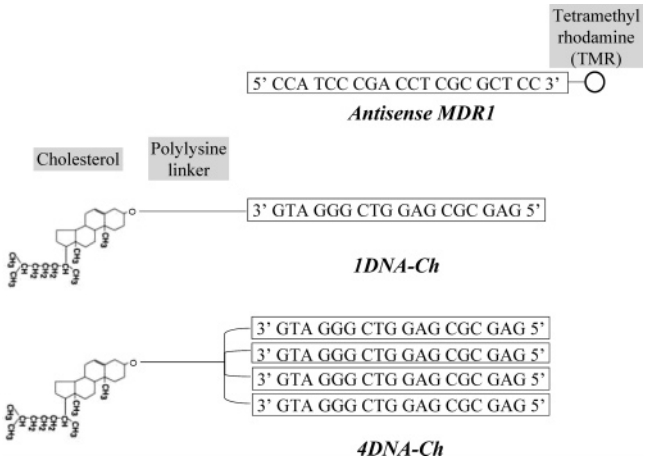

Figure 1. Schematic representation of the structures corresponding to the antisense *MDR1* and cholesterol-modified oligonucleotides (1DNA−Ch and 4DNA−Ch).

Complexation between double-stranded DNA and Lipofectamine (Invitrogen) was done in PBS. Samples were measured after 30 min of incubation by placing a few drops on a glass coverslip cleaned by sonication in acetone, NaOH, and Milli-Q water.

In the setup for single-molecule measurements (for a detailed description, see ref 47), the excitation was performed by a continuous He−Ne laser (543 nm) (05-LGP-193, Melles Griot). The light is directed on the back aperture of an Olympus IX 70 inverted microscope. An oil immersion lens (Zeiss 100×, 1.4 NA) was used. Fluorescence is collected by the same lens, then passed through a dichroic mirror (Chroma Technology, Brattleboro, NY), a notch filter (Kaiser Optical Systems, Ann Arbor, MI), and a long-pass filter (555 nm, Chroma Technology, Brattleboro, NY), and focused on a 100 μm pinhole, corresponding to a selected observation area of 1 μm. The emitted light was collected by an avalanche photodiode, and the detected signal was recorded with a TCSPC PC card (SPC 630, Becker & Hickl Gmbh, Germany) using the FIFO mode (first-in, first-out). Triggering of the card was done by applying a signal from a pulse generator. In this configuration, the time lag between consecutive photons is detected. The stored data are used to reconstruct the fluorescence intensity trace (transient) with a time resolution of 50 ns. Autocorrelation curves were generated using a home-made program and were analyzed in the commercially available Origin program using a fitting function that takes into account contributions of the intersystem crossing (triplet) and one diffusion component (eq 1) or two diffusing components (eq 2)[48,49]

$$G(\tau) = 1 + \frac{1}{N}(1 - T + T\,e^{-(\tau/\tau_{triplet})})\left(\frac{1}{1+\frac{\tau}{\tau_D}}\right)\frac{1}{\left(1+\left(\frac{r_0}{z}\right)^2\frac{\tau}{\tau_D}\right)^{1/2}} \quad (1)$$

$$G(\tau) = 1 + \frac{1}{N}(1 - T + T\,e^{-(\tau/\tau_{triplet})})\left(\left(\frac{1-f}{1+\frac{\tau}{\tau_{D_{DNA}}}}\right)\times \frac{1}{\left(1+\left(\frac{r_0}{z}\right)^2\frac{\tau}{\tau_{D_{DNA}}}\right)^{1/2}} + \left(\frac{f}{1+\frac{\tau}{\tau_{D_{lipoplex}}}}\right)\frac{1}{\left(1+\left(\frac{r_0}{z}\right)^2\frac{\tau}{\tau_{D_{lipoplex}}}\right)^{1/2}}\right) \quad (2)$$

where $G(\tau)$ is the autocorrelation function, N is the number of molecules in the laser focus, T is the triplet fraction, $\tau_{triplet}$ is the lifetime of the triplet state, τ_D is the diffusion time, $\tau_{D_{DNA}}$ is the diffusion time of free DNA, $\tau_{D_{lipoplex}}$ is the diffusion time of lipoplexes, f is the fraction of lipoplexes, r_0 is the radius of the laser focus, and z is half of the long axis of the laser focus.

Calibration of the system was done with sulforhodamine 101 to determine the shape parameter of the laser focus r_0 and then to calculate the diffusion coefficient (D) of DNA

$$D = \frac{r_0^2}{4t} \quad (3)$$

The ratio r_0/z was estimated from the fitting of the autocorrelation curve of sulforhodamine and was used to calculate the confocal volume.

The fluorescence bursts were selected in the same home-made program after filtering the raw data with a Lee filter, as described in the literature.[50]

Results

Calibrating the Microscope. Fluorescence correlation spectroscopy is a method that can provide valuable information in biology,[31,51,52] but data in the literature warn about possible artifacts leading to misinterpretations.[53] The results are influenced by the size of the confocal volume, the light distribution within it, and the mathematical models applied for the curve fitting. When using one-photon excitation, the size of the confocal volume is given by the excitation wavelength, the numerical aperture of the objective lens, and the sizes of the pinholes.[53,54] Typically, high numerical aperture objectives are used, while the pinhole size is generally 50−100 μm, even though pinholes as large as 250 μm were used for some applications.[53−55] It was shown that a large pinhole combined with overfilling the back aperture of the objective lens generates a non-Gaussian distribution of light.[54] The consequence is that the obtained autocorrelation function cannot be fitted with the model taking into account the triplet lifetime and the diffusion time, and an additional component (e.g., chemical kinetics or a second diffusing component) has to be introduced.[54] Furthermore, using an oil immersion lens can also influence the parameters of the confocal volume when the observation is done too far from the coverglass due to the differences in the refractive indices of oil and water.[52]

We tested the experimental conditions using sulforhodamine 101. The diffusion coefficient of the rhodamine derivatives in water was considered to be 2.8×10^{-10} m^2 s^{-1}.[54] The calculations were made with this value because there is not yet a general consensus about the use of a higher value ($\sim 4 \times 10^{-10}$ m^2 s^{-1}) reported for small dyes such as rhodamine or Atto compounds.[56,57] The laser beam was expanded with a telescopic system to obtain the same size as the back aperture of the Zeiss oil immersion lens used. (The ratio β between the radius of the back aperture and the radius of the laser beam was virtually 1, a value within the limits calculated in ref 54 to give a Gaussian light distribution in the focus.) Using an excitation power of 35 μW for the 543 nm wavelength, a pinhole size of 100 μm and working at 4 μm above the coverglass, the radius of the confocal volume was calculated to be $r_0 = 0.3$ μm (according to eq 3). The value for z was estimated from the ratio $\omega = r_0/z$ obtained after fitting the autocorrelation curve and was found to be ~ 2 μm. r_0 and z were used to calculate the observation volume, giving a value of ~ 1.1 fL. Although using an oil immersion lens and a short distance between the coverglass and the focal volume might affect the absolute value of the diffusion coefficients, we are reporting in the paper the relative values of the diffusion coefficients, as obtained after the calibration of the focal volume with rhodamine.

SM Experiments. A similar DNA concentration (2×10^{-8} M) was added to suspensions containing different amounts of Lipofectamine (1.5, 4.9, 8.2, 11.5, and 14.9 μg/mL). Figure 2

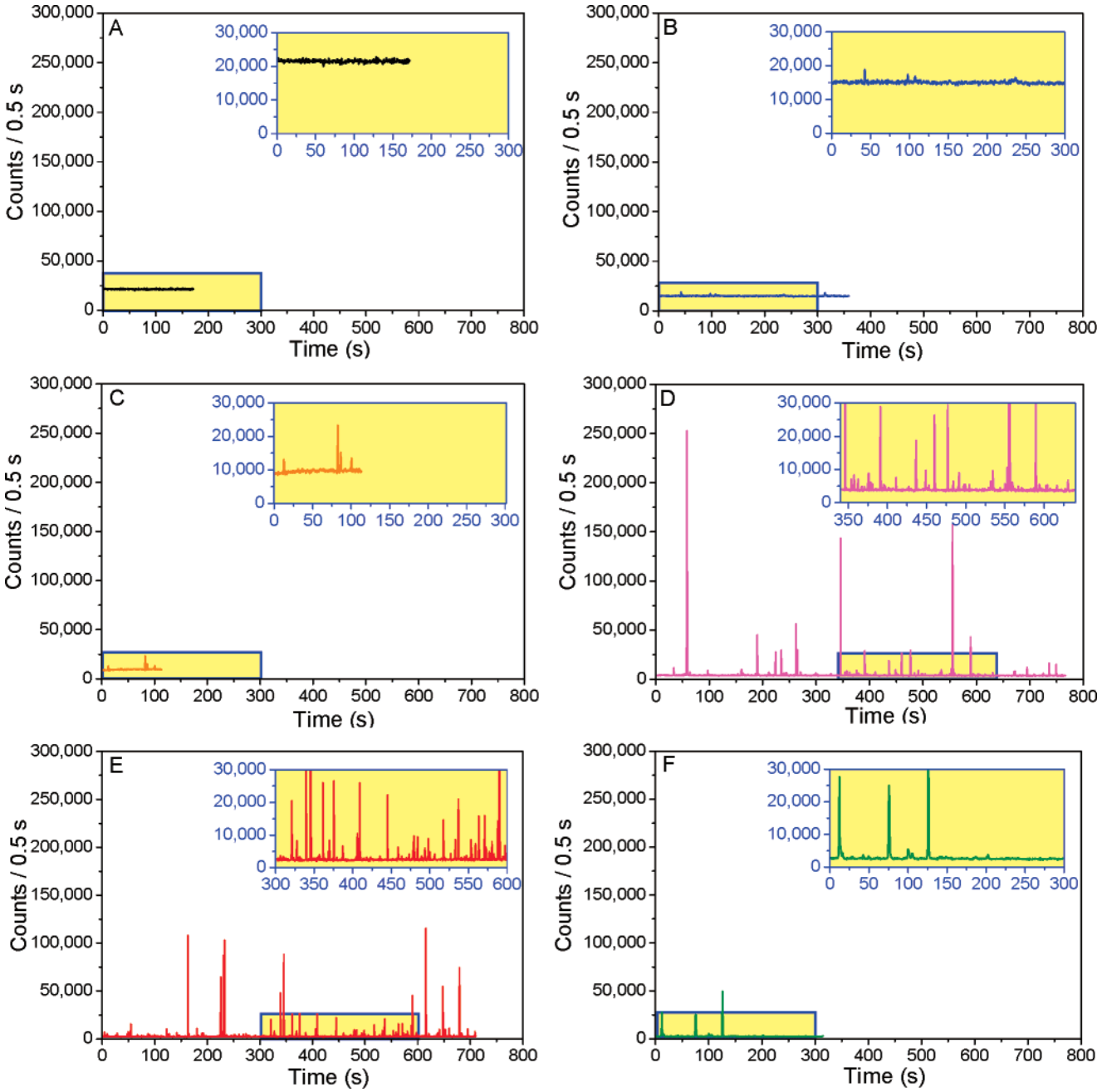

Figure 2. Traces recorded for nonmodified DNA at different Lipofectamine concentrations: (A) 0, (B) 1.5, (C) 4.9, (D) 8.2, (E) 11.5, and (F) 14.9 μg/mL. The insets are obtained by enlarging regions delineated in blue from each trace. All traces are represented on the same scale.

shows the fluorescence intensity traces obtained for the nonmodified DNA. Similar data were recorded for the cholesterol-modified sequences. For the free DNA (no Lipofectamine added), the highest fluorescence intensity level was measured (Figure 2A). Adding the lipids causes a decrease in the baseline intensity level due to the fact that part of the DNA molecules are bound in large complexes (seen as spikes), so there are fewer free oligonucleotides. The higher the lipid concentration, the lower the baseline intensity level, and more spikes are observed (Figures 2B−F).

As explained in the Introduction, the baseline fluorescent levels and the fluorescent bursts were separately analyzed within the same trace.

Autocorrelation curves were constructed for the constant intensity levels between consecutive bursts, using intervals of ~30 s. At least 10 autocorrelation curves were obtained for each data set. The diffusion coefficient and the number of particles present in the laser focus can be determined by fitting the autocorrelation curves. When no Lipofectamine is added to the DNA, the curves were analyzed using the model taking into account only one diffusing component (eq 1). With the previously determined r_0 value of 0.3 μm, *the diffusion coefficient* of the double-stranded DNA was estimated to be $(1.2 \pm 0.1) \times 10^{-10}$ m^2 s^{-1} (according to eq 1). This experimental value was found to be in agreement with the theoretical value of the diffusion coefficient calculated for a rodlike molecule of 7 nm × 2 nm (the approximate size of the double-stranded oligonucleotide with 20 base pairs (bp's)). The theoretical value was 1.0×10^{-10} m^2 s^{-1} and was calculated according to the relation[58]

$$D = \frac{kT\left(\ln\frac{L}{d} + \gamma\right)}{3\pi\eta L} \quad (4)$$

where L is the length of the molecule, d is the molecule's diameter, and $\gamma = 0.38$ (an end-effect correction factor).

No significant differences were observed for the diffusion coefficient of the double strands containing cholesterol-modified sequences compared to the nonmodified DNA. The average values for the diffusion coefficients are $D_1 = (1.1 \pm 0.1) \times 10^{-10}$ m^2 s^{-1} and $D_4 = (1.2 \pm 0.1) \times 10^{-10}$ m^2 s^{-1} for the compounds bearing one and four oligonucleotides, respectively. For spherical particles, a 2 times decrease in the diffusion coefficient value can be observed only if the molecular weight increases 8 times, because of the third power dependence of the diffusion coefficient on the molecular weight according to the Stokes−Einstein relation

$$D = \frac{kT}{6\pi\eta R_h} = \frac{kT}{6\pi\eta\left(\frac{3}{4\pi}\frac{M}{N_A}V\right)^{1/3}} \quad (5)$$

where D is the diffusion coefficient, k is Bolzmann's constant, T is the absolute temperature, η is the viscosity, R_h is the hydrodynamic radius of the particle, M is the molecular weight, N_A is Avogadro's number, and V is the volume of the particle.

Therefore, the molecular weight of the cholesterol-modified sequences does not seem to be high enough to discriminate them from the nonmodified DNA based on their diffusion coefficients.

The triplet contribution was around 33% for all of the analyzed curves, a typical value obtained in FCS measurements for rhodamine dyes.

In the presence of Lipofectamine, most of the autocorrelation curves constructed from the baseline level between bursts were analyzed with one diffusing component (eq 1), which was considered to be the unbound DNA (Figure 3A). However, when 8.2 μg/mL Lipofectamine was used, half of the number of autocorrelation curves obtained for the nonmodified DNA was fitted using a model with two diffusing terms (eq 2). The fact that not all of the curves are fitted with the same model probably reflects the high spatial and temporal heterogeneity of the system at this concentration. This means that lipoplexes with different sizes pass through the confocal volume as a function of time and also that the size of the lipoplexes can change as a function of time if this complex system is not in equilibrium. For 11.5 μg/mL Lipofectamine, the autocorrelation curves for both nonmodified DNA and 1DNA−Ch showed a second diffusing component (Figure 3B). The slower diffusing component was assigned to the presence of small lipoplexes that do not give fluorescent bursts when they are in focus. The values for the second diffusion coefficient are listed in Table 1. Assuming a spherical shape for these lipoplexes, their hydrodynamic radius R_h can be calculated using the Stokes−Einstein relation (eq 5). The average values of the hydrodynamic radii range between 400 and 600 nm (Table 1).

The number of the freely diffusing molecules in the laser focus can be estimated from the amplitude of the autocorrelation curves and is given in Table 2. For a free DNA concentration of 2×10^{-8} M and a confocal volume of ~1.1 fL, there should be ~14 detected molecules. The experimental values are in very good agreement with the calculated one (Table 2, corresponding to 0 μg/mL Lipofectamine concentration). By adding increasing amounts of Lipofectamine, the number of the free DNA molecules decreases (Table 2), because a fraction of them is trapped in lipoplexes. This is also visible in the increased amplitude of the autocorrelation functions due to the fact that this parameter is inversely proportional to the number of particles within the confocal volume (Figure 3A).

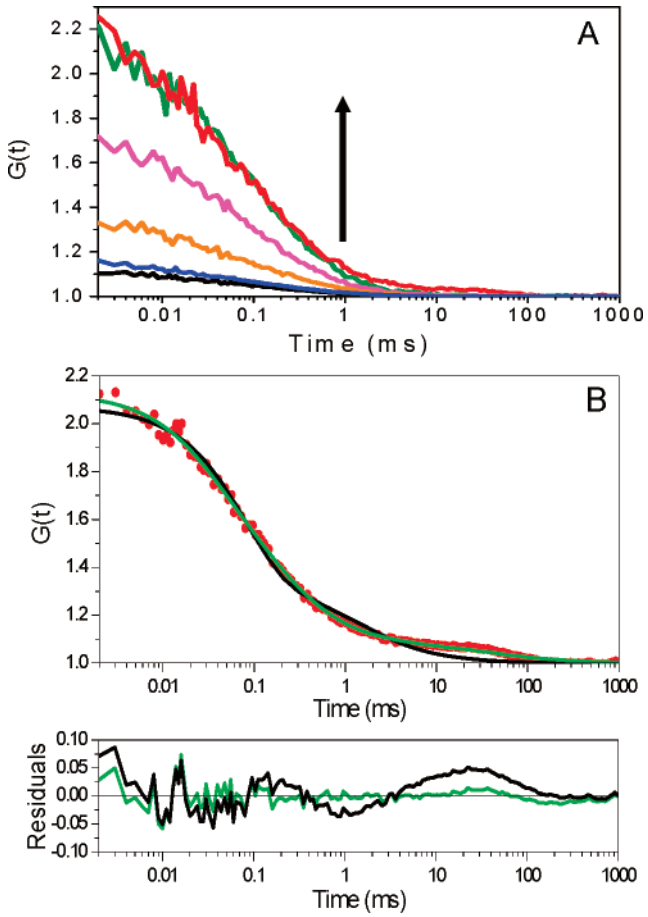

Figure 3. (A) Examples of autocorrelation curves computed for a 30 s time interval on the constant level between bursts for the recorded traces: black, free DNA; blue, DNA and 1.5 μg/mL Lipofectamine; orange, DNA and 4.9 μg/mL Lipofectamine; pink, DNA and 8.2 μg/mL Lipofectamine; red, DNA and 11.5 μg/mL Lipofectamine; green, DNA and 14.9 μg/mL Lipofectamine. The arrow shows the direction of the increase of the Lipofectamine concentration. (B) Example of an autocorrelation curve (red) that could not be fitted with one diffusing component (black) due to the presence of the second component with a small contribution (DNA and 11.5 μg/mL Lipofectamine). The result of two-component fitting is shown in green. The corresponding residuals for one-component fitting (black) and two-component fitting (green) are shown in the bottom panel.

The average values obtained by fitting 10 autocorrelation curves for each data set are listed in Table 2. They were used to calculate the percentage of the bound DNA in lipoplexes (vide infra).

By analyzing *the fluorescent bursts*, information about *the duration* and *the integrated number of counts per burst* can be obtained (Figures 4A−C). These parameters were estimated for three Lipofectamine concentrations (8.2, 11.5, and 14.9 μg/mL). In the presence of 14.9 μg/mL Lipofectamine, bursts longer than 2 s can be observed for all three DNA compounds (Figure 4A), but the integrated number of counts per burst is lower compared to the other Lipofectamine concentrations. When the Lipofectamine concentration is reduced (11.5 μg/mL), most of the bursts last for less than 2 s in the case of 1DNA−Ch and nonmodified DNA (Figure 4B), while long bursts are still observed for 4DNA−Ch. However, the integrated number of counts per burst increases compared to the previous Lipofectamine concentration, especially for the nonmodified DNA. By decreasing further the lipid concentration (8.2 μg/mL), longer bursts with higher integrated numbers of counts are observed for 4DNA−Ch and 1DNA−Ch compared to DNA (Figure 4C).

Table 1. Analysis Results for the Autocorrelation Curves Fitted Using Two Diffusing Components Corresponding to the Free DNA and the Nanometer-Sized Lipoplexes

Lipofectamine concentration (mg/mL)	DNA type	DNA diffusion coefficient ($m^2\ s^{-1}$)	fraction of the second component (%)	second component diffusion coefficient ($m^2\ s^{-1}$)	average hydrodynamic radius (nm)
8.2	DNA	$(1.2 \pm 0.1) \times 10^{-10}$	4.04 ± 2.59	$(3.6 \pm 1.4) \times 10^{-13}$	600 ± 72
11.5	1DNA−Ch	$(1.1 \pm 0.1) \times 10^{-10}$	2.77 ± 0.60	$(3.9 \pm 1.8) \times 10^{-13}$	575 ± 195
11.5	DNA	$(1.2 \pm 0.1) \times 10^{-10}$	5.24 ± 2.41	$(4.9 \pm 0.5) \times 10^{-13}$	430 ± 136

Table 2. Average Number of Freely Diffusing DNA Molecules in the Laser Focus at Different Lipofectamine Concentrations

Lipofectamine concentration (μg/mL)	DNA	1DNA−Ch	4DNA−Ch
0	13.5 ± 0.3	15.8 ± 0.5	14.7 ± 0.6
1.5	10.9 ± 1.9	11.2 ± 0.5	14.8 ± 1.2
4.9	4.2 ± 0.4	5.8 ± 0.4	8.7 ± 0.7
8.2	1.7 ± 0.1	2.9 ± 0.1	4.6 ± 0.3
11.5	1.0 ± 0.1	2.3 ± 0.1	1.7 ± 0.1
14.9	1.0 ± 0.1	1.4 ± 0.1	1.2 ± 0.1

One can assume that the longer the burst duration, the larger the particle diameter. The sizes of lipoplexes with diffusion times on the order of seconds are in the micrometer range, but for a very precise calculation of their hydrodynamic radius, corrections would have to be applied because the particles are not infinitely small compared to the diameter of the laser focus.[59] However, bursts with high integrated numbers of fluorescence counts contain high numbers of DNA molecules. To qualitatively estimate the proportion of Lipofectamine and DNA in different lipoplexes, the integrated number of counts per burst was divided by the duration of the burst, and the corresponding histograms were constructed (Figures 4D−F). One can observe that the complexes with the highest integrated number of counts for a given size (i.e., diffusion time) correspond to the lower Lipofectamine concentration for all three DNA types (pink lines in Figures 4D−F). The integrated number of counts normalized for the burst duration decreases as the Lipofectamine concentration increases. This means that the complexes contain less DNA and more lipids as the concentration of Lipofectamine increases.

It is significant to note the presence of very long bursts in the case of 4DNA−Ch for all three Lipofectamine concentrations shown in Figures 4A−C.

Information about *the number of DNA molecules bound in one complex* can be obtained from the SM data. Inspection of the fluorescence intensity traces (Figure 2) shows a very high heterogeneity regarding the peak number of counts for different spikes, in agreement with the data from literature about the inhomogeneity of lipoplex size and composition.[6,11,20] After determining the number of free oligonucleotides from the amplitudes of the autocorrelation curves, the number of counts per molecule can be calculated by dividing the value of the baseline intensity level by the number of free DNA molecules. The peak count rate of the bursts is then divided to the number of counts per molecule obtained from the baseline level in the same trace to estimate the number of DNA molecules trapped in one large complex. Similar values were obtained for all three DNA types. For example, the number of DNA molecules contained in complexes that give a peak count rates of 250 000 counts/0.5 s is ~115, for complexes with 100 000 counts/0.5 s in the peak there are ~50 DNA molecules, and for the ones with 20 000 counts/0.5 s in the peak, ~10 DNA oligonucleotides are present. In these estimations, one has to keep in mind that the large complexes do not always pass through the middle of the laser focus and also that the excitation profile is not homogeneous. Furthermore, self-quenching or singlet−singlet annihilation between the rhodamine molecules brought in close proximity by DNA condensation in lipoplexes can take place. All of these factors will reduce the detected fluorescence intensity, and therefore the real number of molecules within these lipoplexes can be even higher.

In samples with a high degree of polydispersity, such as lipoplex suspensions, one could expect to find particles with micrometer sizes that determine bursts in the fluorescent trace (Figures 2B−F), aggregates with a diameter of a few hundreds of nanometers discriminated in the baseline level by their long diffusion times (Figure 3B and Table 1), and even smaller molecular clusters containing few DNA strands. In the last case, if their molecular weight is not at least 8 times higher than that of the DNA double strand, then they cannot be differentiated from the free DNA based on their diffusion coefficients (eq 5).

When different species cannot be discriminated in FCS based on their diffusion coefficients, a different strategy consists of analyzing the amplitudes of the fluorescence fluctuations instead of the time scale of the diffusion processes, provided that the analyzed species have different brightnesses (as in the cases of dimers or small oligomers). A first method proposed[35,36] is the calculation of the amplitudes of the high-order autocorrelation function. From this analysis, the concentrations of monomers and oligomers as well as the average oligomerization factor (i.e., the number of monomers in an aggregate) can be obtained. Another approach is the analysis of fluctuation moments,[37] in which the *n*th power of the fluorescence fluctuation values is calculated, resulting in very large values of the fluctuation moments corresponding to aggregates and allowing their discrimination from the free monomers. More recently, the photon counting histogram (PCH)[38] and the fluorescence intensity distribution analysis (FIDA)[39] were proposed. Both methods, even though developed independently, consist of successively convoluting the photon count distributions of each species with those of the other species. In this way, it is possible to determine the concentration and the brightness for more than two species with different brightnesses and/or numbers of monomers.

To check for the presence of lipoplexes formed with only a few DNA molecules that could not be detected as a second diffusing component in the baseline fluorescence of the recorded traces, *the amplitudes of the high-order autocorrelation curves* were calculated for the constant levels between bursts according to the method described by Palmer and Thompson.[35] The high-order fluorescence autocorrelation function is defined as

$$G_{ij}(\tau) = \frac{\langle \delta F^i(t+\tau)\delta F^j(t)\rangle - \langle \delta F^i(t)\rangle\langle \delta F^j(t)\rangle}{\langle F(t)\rangle^{i+j}} \qquad (6)$$

where $F(t)$ is the recorded fluorescence signal, $\delta F(t) = F(t) - \langle F(t)\rangle$ is the fluctuation of the fluorescence at time t from its

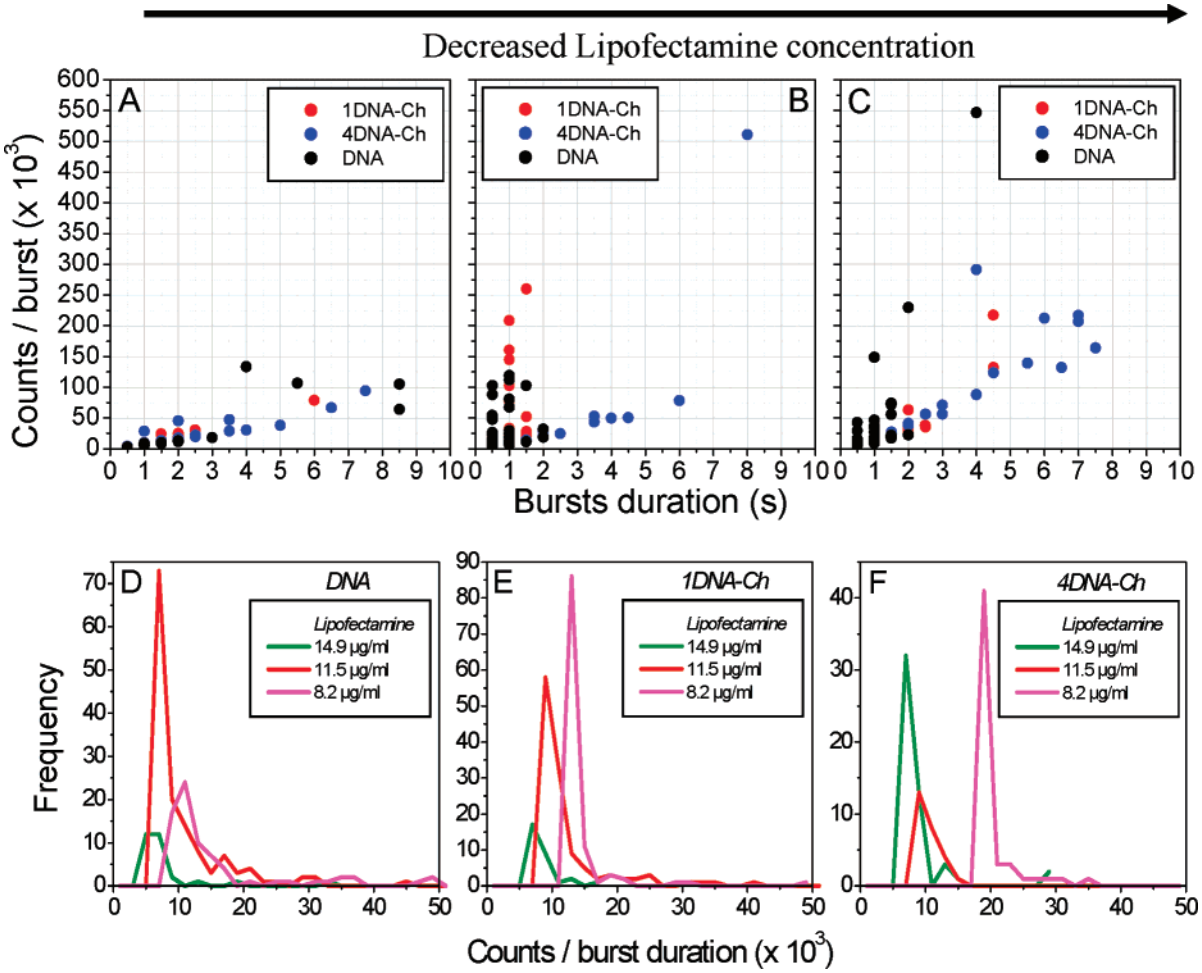

Figure 4. (A−C) Scatter plots for the duration of bursts and the integrated number of counts per bursts obtained for three Lipofectamine concentrations: (A) 14.9, (B) 11.5, and (C) 8.2 μg/mL. (D−E) Histograms obtained by dividing the integrated number of fluorescent counts per burst by the duration of the burst for (D) nonmodified DNA, (E) 1DNA−Ch, and (F) 4DNA−Ch.

average value, i and j are integers, and $\langle\cdots\rangle$ denotes thermodynamic ensemble average.

The values of the total concentration of monomers C_t of the fraction of monomers present in oligomeric form f and of the oligomerization factor α can be obtained as a solution of a system of nonlinear equations

$$\begin{cases} \dfrac{G_{11}(0)}{\gamma_2} = (1 - f + \alpha f)/C_t \\ \dfrac{G_{12}(0)}{\gamma_3} = (1 - f + \alpha^2 f)/C_t^2 \\ \dfrac{G_{13}(0) - 3G_{11}^2(0)}{\gamma_4} = (1 - f + \alpha^3 f)/C_t^3 \end{cases} \quad (7)$$

where

$$\gamma_n = \frac{\int w^n(\vec{\mathbf{r}})\, dV}{(\int w(\vec{\mathbf{r}})\, dV)^n} \quad (n = 2, 3, 4) \quad (8)$$

and $w(\vec{\mathbf{r}})$ denotes the product of the excitation intensity spatial distribution and the light-detection spatial distribution.

The values of γ_n were numerically computed assuming a three-dimensional Gaussian profile of function $w(\vec{\mathbf{r}})$.[60] High-order fluorescence fluctuation autocorrelation functions $G_{ij}(t)$ were calculated from the detected fluorescence transients, which were discretized with time bins of 100 μs. The values of $G_{ij}(0)$ were found by extrapolation of functions $G_{ij}(t)$ to the zero time point. Next, an appropriate correction for special high-order effects caused by detection efficiency and background presence was carried out.

After determining the values of α, f, and C_t, one can easily calculate the monomer concentration C_m and the oligomer concentration C_o using the following expressions

$$C_m = C_t(1 - f) \quad (9)$$

$$C_o = C_t f/\alpha \quad (10)$$

For 1.5 μg/mL Lipofectamine, the oligomerization factor α was around 1, meaning that there are only free DNA molecules diffusing. The low DNA-containing complexes are observed starting from 4.9 μg/mL Lipofectamine for the nonmodified DNA and from 8.2 μg/mL Lipofectamine for the cholesterol-modified sequences (Table 3). The oligomerization number is generally less than 8, explaining the fact that these lipoplexes could not be detected by their diffusion coefficient.

The detected errors are quite large, probably because of both spatial and temporal heterogeneity of the system, as previously discussed.

The percentage of the bound DNA was calculated by comparing the number of particles obtained from each autocorrelation curve (free DNA) with the total number of DNA particles obtained when no lipids were added (Table 2), given the fact that the DNA concentration was constant in these experiments. The concentration of lipoplexes containing ap-

Table 3. Parameters Obtained from the Analysis of the Amplitudes of the High-Order Autocorrelation Curves[30] [a]

Lipofectamine concentration (μg/mL)	parameters	1DNA−Ch	4DNA−Ch	DNA
1.5	α	≤ 1	≤ 1	≤ 1
4.9	f			$(2.8 \pm 0.8) \times 10^{-1}$
	α	≤ 1	≤ 1	6.3 ± 1.5
	C_o			$(3.3 \pm 1.3) \times 10^{-1}$
	C_m			5.1 ± 1.6
8.2	f	$(1.7 \pm 1.0) \times 10^{-1}$	$(2.8 \pm 2.1) \times 10^{-1}$	$(2.7 \pm 1.4) \times 10^{-1}$
	α	6.2 ± 1.3	10.0 ± 5.3	7.1 ± 0.8
	C_o	$(1.0 \pm 0.7) \times 10^{-1}$	$(3.9 \pm 3.7) \times 10^{-1}$	$(1.1 \pm 0.8) \times 10^{-1}$
	C_m	2.5 ± 0.2	5.7 ± 1.3	1.8 ± 0.4
11.5	f	$(2.3 \pm 1.1) \times 10^{-1}$	$(3.7 \pm 1.9) \times 10^{-1}$	$(3.9 \pm 1.7) \times 10^{-1}$
	α	7.0 ± 1.7	8.9 ± 2.2	7.0 ± 1.8
	C_o	$(1.1 \pm 0.6) \times 10^{-1}$	$(1.5 \pm 1.3) \times 10^{-1}$	$(1.1 \pm 0.5) \times 10^{-1}$
	C_m	2.7 ± 0.9	1.8 ± 0.2	1.1 ± 0.1
14.9	f		$(2.1 \pm 0.6) \times 10^{-1}$	$(0.8 \pm 0.6) \times 10^{-1}$
	α	≤ 1	7.5 ± 0.7	10.0 ± 4.2
	C_o		$(0.5 \pm 0.2) \times 10^{-1}$	$(1.0 \pm 0.9) \times 10^{-2}$
	C_m		1.4 ± 0.1	$(8.6 \pm 0.4) \times 10^{-1}$

[a] f = oligomers fraction; α = oligomerization factor (number of monomers in an aggregate); C_m = monomer concentration (expressed as number of molecules in the confocal volume); C_o = oligomers concentration (expressed as number of molecules in the confocal volume).

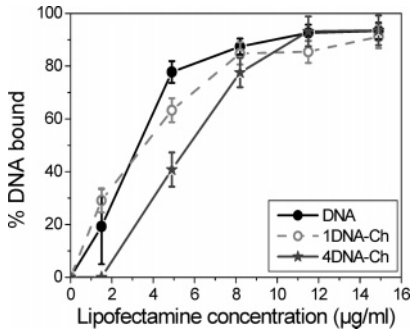

Figure 5. Percentage of bound DNA determined from SM experiments.

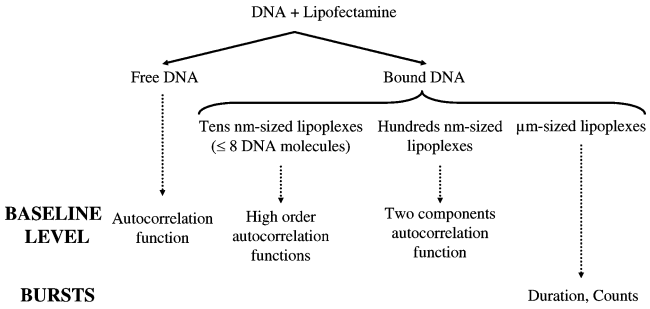

Figure 6. Schematic representation of the information extracted using different analysis methods from the fluorescent traces recorded for DNA in the presence of cationic lipids.

proximately eight DNA molecules (obtained from the high-order autocorrelation functions) was used to correct the values. The percentage of the bound DNA as a function of the Lipofectamine concentration is represented in Figure 5. As more Lipofectamine is added, the percentage of DNA bound in lipoplexes increases. There are no significant differences between the nonmodified double-stranded DNA and 1DNA−Ch. For the compound bearing four oligonucleotides attached to cholesterol, a slow increase of the bound fraction is observed for small Lipofectamine concentrations, but this fraction reaches in the end similar values as for the other two compounds.

Discussion

The differences in lipoplex formation for normal and cholesterol-modified oligonucleotides have been investigated by means of SM fluorescence spectroscopy. Using a simple experimental scheme in which only the DNA is fluorescently labeled, multiple pieces of information could be simultaneously obtained from these measurements by recording data with a time correlated single photon counting setup developed for SM experiments and by separately analyzing the baseline fluorescence intensity level and the fluorescent bursts (Figure 6).

The autocorrelation functions constructed only with the photons selected from the constant intensity levels between bursts can be analyzed with routine models, allowing the determination of diffusion coefficients and of the number of particles in the laser focus, as usually done in FCS. By using the same DNA concentration in all samples and adding increasing amounts of cationic lipids, the decrease of the fluorescence baseline levels (Figures 2A−F) and the corresponding increase of the amplitudes of the autocorrelation function (Figure 3A) can be observed. They are consequences of the reduction of the number of freely diffusing DNA molecules. The presence of the free DNA is confirmed by the characteristic value of its diffusion coefficient. Lipoplexes hundreds of nanometers in size could be discriminated in the baseline level based on their longer diffusion coefficients compared to the free DNA (Figure 3B and Table 1). A puzzling observation is that we could not discriminate in all of the baseline levels the free DNA and the nanometer-sized lipoplexes based on distinct diffusion times. One would expect that the binding of small oligonucleotides (20 bp's) to a lipid vesicle should significantly increase the DNA diffusion time.[48] Lipofectamine is a 3:1 (w/w) mixture of 2,3-dioleoyloxy-*N*-[2(sperminecarboxamido)ethyl]-*N*,*N*-dimethyl-1-propanaminium trifluoroacetate (DOSPA) and dioleoyl phosphatidylethanolamine (DOPE). Due to its large polar group, DOSPA favors the formation of micelles,[6] and DOPE (in a lower quantity) cannot compensate for this tendency to form a lamellar phase (lipo-

somes). Indeed, measurements using quasi-elastic light scattering of Lipofectamine particles indicate that their size is less than 5 nm, which corresponds to micelles rather than to liposomes.[61] When a mixture of DOSPA/DOPE is used, the presence of very small DNA−lipid particles (5−10 nm) coexisting with large lipoplexes was demonstrated by cryo-transmission electron microscopy.[7] Considering an average of 70 Å^2 for the cross-sectional area per lipid molecule,[6] this means that there are less than 100 lipid molecules in such a micelle. As a consequence, it is possible that the molecular weight of a micelle is not 8 times higher than that of the DNA sequences that were used, so they cannot be distinguished by different diffusion times. However, a higher diffusion coefficient for DNA−liposomes can be expected only if the vesicles are not destabilized after the interaction. It was proposed[11,20] that fast mixing of DNA with small unilamellar vesicles occurs by preserving their integrity in a first step, followed by their disruption and aggregation, but the authors recognize that the formation of lipoplexes from micellar cationic lipids may occur through a different mechanism. The presence of these very small particles containing generally ≤8 DNA molecules was concluded from the analysis of the high-order autocorrelation curves calculated also from the baseline level of the fluorescent traces (Table 3).

Lipoplexes with micrometer sizes are observed as fluorescent bursts in the recorded traces (Figures 2C−F). Using SM measurements, each micrometer-sized particle passing through the focal volume can be analyzed. The duration of the burst depends on the lipoplex size, and the intensity of the burst is dependent on the number of DNA molecules trapped in the complex. The analysis in Figures 4D−F allows us to estimate the relative proportions of DNA and lipids in lipoplexes. By increasing the Lipofectamine concentration, particles with a given size contain less DNA and more lipid molecules. However, a precise quantification of lipids in each particle should be done by fluorescently labeling the vesicles[20] or by FRET−FCS.[62] The maximum number of the DNA molecules in one lipoplex was found to be in our case around 100, while for lipoplexes formed from the association of a 40 bp oligonucleotide with cationic liposomes containing only 1,2-dioleoyl-3-trimethylammonium propane (DOTAP) this is approximately 2000.[20] The difference could be related to the small sizes of the Lipofectamine particles (as previously discussed) because it was demonstrated that the sizes of lipoplexes are determined by the initial size of the lipid particles.[11]

The maximum heterogeneity was observed for all of the analyzed oligonucleotides when 11.5 μg/mL Lipofectamine is used: Micrometer-sized lipoplexes appearing as numerous large or small spikes coexist with tens to hundreds of nanometer-sized lipoplexes. This can be an indication of a very high instability of lipoplexes, which was correlated with high transfection efficiency in vivo.[7,63] When an excess of DNA or lipids is present, the complexes are reported to be larger and more stable.[6] Our experimental data indicate indeed that for DNA plus 8.2 and 14.9 μg/mL Lipofectamine there are more lipoplexes with longer diffusion times for 1DNA−Ch and normal DNA than for 11.5 μg/mL Lipofectamine (Figures 4A−C).

The explanation for the reduced binding of 4DNA−Ch detected at low Lipofectamine concentrations is not yet obvious. It is possible that due to the electrostatic attraction of four nearby oligonucleotides more Lipofectamine is bound to the same molecule, while other molecules are not condensed. Alternatively, we cannot completely exclude that what we consider "free" DNA is in fact one molecule condensed with few lipids that cannot be identified by a different diffusion time or by the amplitude of the fluorescence intensity fluctuations. (Aggregation is prevented when there are not enough lipids to compensate for the negative charges, and repulsive forces between DNA strands dominate.[64]) However, for 11.5 and 14.9 μg/mL Lipofectamine, no significant differences are observed between the three DNA types. Another finding for 4DNA−Ch relates to the longer diffusion times (i.e., very large lipoplexes) detected for the three ratios considered in Figures 4A−C, as compared to those of the other two compounds. This can be due to the fact that at high enough Lipofectamine concentrations four oligonucleotides are simultaneously immobilized in one complex, generating larger lipoplexes. An explanation for the higher transfection efficiency previously reported by our group for this compound[44] can thus be provided, because the results in the literature indicate that using particles with large sizes increases the transfection efficiency.[11,12,65]

One possible problem when using fluorescence fluctuation analysis is the necessity to have only a few molecules in the detection volume. Therefore, the tested concentrations are in the nanomolar range, while relevant concentrations for living cells can go up to micromolar. Therefore, the equilibrium of the association reaction can be shifted, and the results cannot be extrapolated directly to cellular experiments. One way to overcome this problem is to use a mixture of labeled and nonlabeled reagents to achieve the same concentrations as for transfection[36] or the use of even smaller detection volumes that allow working with higher fluorescent molecule concentrations.[66−68]

Conclusions

We demonstrated that, when quantifying lipoplex formation, SM fluorescence techniques could provide information that is usually obtained only by combining complementary methods in ensemble measurements. SM techniques are particularly useful when highly heterogeneous systems are investigated. By using a single photon counting PC card developed for single-molecule experiments instead of a hardware autocorrelator, data analysis is more flexible. By separately analyzing the baseline fluorescence levels, the number of free and bound DNA molecules, the presence of tens to of hundreds of nanometer-sized lipoplexes could be estimated by applying various mathematical models. The analysis of the fluorescent bursts gave indications about the sizes of the micrometer-sized lipoplexes, the number of DNA molecules present in these large aggregates, and the relative amounts of lipids in each aggregate. In our experiments, the fluorescence intensity of one chromophore was detected in one channel, but in SM measurements more options in designing the experiments are possible (i.e., detection of lifetime, anisotropy, or energy transfer).

A quantitative comparison between three types of DNA could also be done, and a possible explanation for the previously observed higher transfection efficiency of 4DNA−Ch was found in relation to the larger sizes of the aggregates. As suggested by other studies,[43] the main advantage of the cholesterol modification will be the possibility of using other lipid formulations for transfection instead of the cationic derivatives, which possess a higher toxicity.

Acknowledgment. Financial support from the KULeuven research fund (GOA 2/01 and 2/06, Centers of Excellence INPAC and CECAT, IDO/02/014), the Federal Science Policy of Belgium (Grant No. IAP-VI/27), and the Institute for the Promotion of Innovation by Science and Technology in Flanders

(IWT) is acknowledged. This work, as part of the European Science Foundation EUROCORES Programme SONS, was partly supported from funds by the FWO and the EC Sixth Framework Programme, under Contract No. ERAS-CT-2003-980409.

References and Notes

(1) Wasungu, L.; Hoekstra, D. Cationic lipids, lipoplexes and intracellular delivery of genes. *J. Controlled Release* **2006**, *116*, 255−264.

(2) Schmidt-Wolf, G. D.; Schmidt-Wolf, I. G. H. Non-viral and hybrid vectors in human gene therapy: An update. *Trends Mol. Med.* **2003**, *9*, 67−72.

(3) Zuhorn, I. S.; Hoekstra, D. On the mechanism of cationic amphiphile-mediated transfection. To fuse or not to fuse: Is that the question? *J. Membr. Biol.* **2002**, *189*, 167−179.

(4) Uherek, C.; Wels, W. DNA-carrier proteins for targeted gene delivery. *Adv. Drug Delivery Rev.* **2000**, *44*, 153−166.

(5) May, S.; Ben-Shaul, A. Modeling of cationic lipid−DNA complexes. *Curr. Med. Chem.* **2004**, *11*, 151−167.

(6) Simberg, D.; Weisman, S.; Talmon, Y.; Barenholz, Y. DOTAP (and other cationic lipids): Chemistry, biophysics and transfection. *Crit. Rev. Ther. Drug Carrier Syst.* **2004**, *21*, 257−317.

(7) Simberg, D.; Danino, D.; Talmon, Y.; Minsky, A.; Ferrari, E.; Wheeler, C. J.; Barenholz, Y. Phase behavior, DNA ordering, and size instability of cationic lipoplexes. Relevance to optimal transfection activity. *J. Biol. Chem.* **2001**, *276*, 47453−47459.

(8) Rädler, J. O.; Koltover, I.; Salditt, T.; Safinya, C. R. Structure of DNA−cationic liposome complexes: DNA intercalation in multilamellar membranes in distinct interhelical packing regimes. *Science* **1997**, *275*, 810−814.

(9) Koltover, I.; Salditt, T.; Rädler, J. O.; Safinya, C. An inverted hexagonal phase of cationic liposome−DNA complexes related to DNA release and delivery. *Science* **1998**, *281*, 78−81.

(10) Meidan, V. M.; Glezer, J.; Amariglio, N.; Cohen, J. S.; Barenholz, Y. Oligonucleotide lipoplexes: The influence of oligonucleotides composition on complexation. *Biochim. Biophys. Acta* **2001**, *1568*, 177−182.

(11) Rakhmanova, V. A.; Pozharski, E. V.; MacDonald, R. C. Mechanism of lipoplex formation: Dependence of the biological properties of transfection complexes on formulation procedures. *J. Membr. Biol.* **2004**, *200*, 35−45.

(12) Almofti, M. R.; Harashima, H.; Shinohara, Y.; Almofti, A.; Baba, Y.; Kiwada, H. Cationic liposome-mediated gene delivery: Biophysical study and mechanism of internalization. *Arch. Biochem. Biophys.* **2003**, *410*, 246−253.

(13) Simberg, D.; Weisman, S.; Talmon, Y.; Faerman, A.; Shoshani, T.; Barenholz, Y. The role of organ vascularization and lipoplex−serum initial contact in intravenous murine lipofection. *J. Biol. Chem.* **2003**, *278*, 39858−39865.

(14) Madeira, C.; Loura, L. M. S.; Aires-Barros, M. R.; Fedorov, A.; Prieto, M. Characterization of DNA/lipid complexes by fluorescence resonance energy transfer. *Biophys. J.* **2003**, *85*, 3106−3119.

(15) Zelphati, O.; Szoka, F. C., Jr. Mechanism of oligonucleotide release from cationic liposomes. *Proc. Natl. Acad. Sci. U.S.A.* **1996**, *93*, 11493−11498.

(16) Geall, A. J.; Blagbrough, I. S. Rapid and sensitive ethidium bromide fluorescence quenching assay of polyamine conjugate−DNA interactions for the analysis of lipoplex formation in gene therapy. *J. Pharm. Biomed.* **2000**, *22*, 849−859.

(17) Ferrari, M. E.; Rusalov, D.; Enas, J.; Wheeler, C. J. Trends in lipoplex physical properties depend on cationic lipid structure, vehicle and complexation procedure do not correlate with biological activity. *Nucleic Acids Res.* **2001**, *29*, 1539−1548.

(18) Xu, Y.; Hui, S.-W.; Frederik, P.; Szoka, C., Jr. Physicochemical characterization and purification of cationic lipoplexes. *Biophys. J.* **1999**, *77*, 341−353.

(19) Jurkiewicz, P.; Okruszek, A.; Hof, M.; Langner, M. Associating oligonucleotides with positively charged liposomes. *Cell. Mol. Biol. Lett.* **2003**, *8*, 77−84.

(20) Merkle, D.; Lees-Miller, S. P.; Cramb, D. T. Structure and dynamics of lipoplex formation examined using two-photon fluorescence cross-correlation spectroscopy. *Biochemistry* **2004**, *43*, 7263−7272.

(21) Remaut, K.; Lucas, B.; Braeckmans, K.; Sanders, N. N.; Demeester, J.; De Smedt, S. C. Protection of oligonucleotides against nucleases by pegylated and non-pegylated liposomes as studied by fluorescence correlation spectroscopy. *J. Controlled Release* **2005**, *110*, 212−226.

(22) Gordon, S. P.; Berezhna, S.; Scherfeld, D.; Kahya, N.; Schwille, P. Characterization of interaction between cationic lipid−oligonucleotide complexes and cellular membrane lipids using confocal imaging and fluorescence correlation spectroscopy. *Biophys. J.* **2005**, *88*, 305−316.

(23) Berezhna, S.; Schaefer, S.; Heintzmann, R.; Jahnz, M.; Boese, G.; Deniz, A.; Schwille, P. New effects in polynucleotide release from cationic lipid carriers revealed by confocal imaging, fluorescence cross-correlation spectroscopy and single particle tracking. *Biophys. Biochim. Acta* **2005**, *1669*, 193−207.

(24) Van Rompaey, E.; Chen, Y.; Müller, J. D.; Gratton, E.; Van Craenenbroeck, E.; Engelborghs, Y.; De Smedt, S.; Demeester, J. Fluorescence fluctuation analysis for the study of interactions between oligonucleotides and polycationic polymers. *Biol. Chem.* **2001**, *382*, 379−386.

(25) Lucas, B.; Van Rompaey, E.; De Smedt, S. C.; Demeester, J.; Van Oostveldt, P. Dual color fluorescence fluctuation spectroscopy to study the complexation between poly-L-lysisne and oligonucleotides. *Macromolecules* **2002**, *35*, 8152−8160.

(26) Lucas, B.; Remaut, K.; Braeckmans, K.; Haustraete, J.; De Smedt, S. C.; Demeester, J. Studying pegylated DNA complexes by dual color fluorescence fluctuation spectroscopy. *Macromolecules* **2004**, *37*, 3832−3840.

(27) Clamme, J. P.; Azoulay, J.; Mély, Y. Monitoring of the formation and dissociation of polyethilenimine/DNA complexes by two photon fluorescence correlation spectroscopy. *Biophys. J.* **2003**, *84*, 1960−1968.

(28) Remaut, K.; Lucas, B.; Braeckmans, K.; Sanders, N. N.; De Smedt, S. C.; Demeester, J. FRET-FCS as a tool to evaluate the stability of oligonucleotide drugs after intracellular delivery. *J. Controlled Release* **2005**, *103*, 259−271.

(29) De Smedt, S. C.; Remaut, K.; Lucas, B.; Braeckmans, K.; Sanders, N. N.; Demeester, J. Studying biophysical barriers to DNA delivery by advanced light microscopy. *Adv. Drug Delivery Rev.* **2005**, *57*, 191−210.

(30) Elson, E. L. Fluorescence correlation spectroscopy measures molecular transport in cells. *Traffic* **2001**, *2*, 789−796.

(31) Haustein, E.; Schwille, P. Ultrasensitive investigations of biological systems by fluorescence correlation spectroscopy. *Methods* **2003**, *29*, 153−166.

(32) Gösch, M.; Rigler, R. Fluorescence correlation spectroscopy of molecular motions and kinetics. *Adv. Drug Delivery Rev.* **2005**, *57*, 169−190.

(33) Van Craenenbroeck, E.; Vercammen, J.; Matthys, G.; Beirlant, J.; Marot, C.; Hoebeke, J.; Strobbe, R.; Engelborghs, Y. Heuristic statistical analysis of fluorescence fluctuation data with bright spikes: Application to ligand binding to the human serotonin receptor expressed in *Escherichia coli* cells. *Biol. Chem.* **2001**, *382*, 355−361.

(34) Vercammen, J.; Maertens, G.; Gerard, M.; De Clercq, E.; Debyser, Z.; Engelborghs, Y. DNA-induced polymerization of HIV-1 integrase analyzed with fluorescence fluctuation spectroscopy. *J. Biol. Chem.* **2002**, *277*, 38045−38052.

(35) Palmer, A. G.; Thompson, N. L. High-order fluorescence fluctuation analysis of model protein clusters. *Proc. Natl. Acad. Sci. U.S.A.* **1989**, *86*, 6148−6152.

(36) Thompson, N. L.; Mitchell, J. L. High order autocorrelation in fluorescence correlation spectroscopy. In *Fluorescence Correlation Spectroscopy*; Rigler, R., Elson, E. S., Eds.; Springer: Germany, 2001; pp 439−458.

(37) Qian, H.; Elson, E. L. Distribution of molecular aggregation by analysis of fluctuation moments. *Proc. Natl. Acad. Sci. U.S.A.* **1990**, *87*, 5479−5483.

(38) Chen, Y.; Müller, J. D.; So, P. T. C.; Gratton, E. The photon counting histogram in fluorescence fluctuation spectroscopy. *Biophys. J.* **1999**, *77*, 553−567.

(39) Kask, P.; Palo, K.; Ullmann, D.; Gall, K. Fluorescence-intensity distribution analysis and its application in biomolecular detection technology. *Proc. Natl. Acad. Sci. U.S.A.* **1999**, *96*, 13756−13761.

(40) Wahl, M.; Gregor, I.; Patting, M.; Enderlein, J. Fast calculation of fluorescence correlation data with asynchronous time-correlated single-photon counting. *Opt. Express* **2003**, *11*, 3583−3591.

(41) Ozben, T. Mechanism and strategies to overcome multiple drug resistance in cancer. *FEBS Lett.* **2006**, *580*, 2903−2909.

(42) Astriab-Fisher, A.; Fisher, M. H.; Juliano, R.; Herdewijn, P. Increased uptake of antisense oligonucleotides by delivery as double stranded complexes. *Biochem. Pharmacol.* **2004**, *68*, 403−407.

(43) Krieg, A. M.; Tonkinson, J.; Matson, S.; Zhao, M.; Saxon, M.; Zhang, L.-M.; Bhanja, U.; Yakubov, L.; Stein, C. A. Modification of antisense phosphodiester oligodeoxynucleotides by a 5′ cholesteryl moiety increases cellular association and improves efficiency. *Proc. Natl. Acad. Sci. U.S.A.* **1993**, *90*, 1048−1052.
(44) Chaltin, P.; Margineanu, A.; Marchand, D.; Van Aerschot, A.; Rozenski, J.; De Schryver, F.; Juliano, R.; De Feyter, S.; Herdewijn, P. Delivery of antisense oligonucleotide using cholesterol-modified sense dendrimers and cationic lipids. *Bioconjugate Chem.* **2005**, *16*, 827−836.
(45) Astriab-Fisher, A.; Sergueev, D. S.; Fisher, M.; Ramsay Shaw, B.; Juliano, R. L. Antisense inhibition of P-glycoprotein expression using peptide−oligonucleotide conjugates. *Biochem. Pharmacol.* **2000**, *60*, 83−90.
(46) Cavaluzzi, M. J.; Borer, P. N. Revised UV extinction coefficients for nucleoside-5′-monophosphates and unpaired DNA and RNA. *Nucleic Acids Res.* **2004**, *32*, e13.
(47) Cotlet, M.; Hofkens, J.; Habuchi, S.; Dirix, G.; Van Guyse, M.; Michiels, J.; Vanderleyden, J.; De Schryver, F. C. Identification of different emitting species in the red fluorescent protein DsRed by means of ensemble and single molecule spectroscopy *Proc. Natl. Acad. Sci. U.S.A.* **2001**, *98*, 14398−14403.
(48) Pramanik, A.; Thyberg, P.; Rigler, R. Molecular interactions of peptides with phospholipids vesicle membranes as studied by fluorescence correlation spectroscopy. *Chem. Phys. Lipids* **2000**, *104*, 35−47.
(49) Schwille, P.; Kummer, S.; Heikal, A. A.; Moerner, W. E.; Webb, W. W. Fluorescence correlation spectroscopy reveals fast optical excitation-driven intramolecular dynamics of yellow fluorescent proteins. *Proc. Natl. Acad. Sci. U.S.A.* **2000**, *97*, 151−156.
(50) Enderlein, J.; Robbins, D. L.; Ambrose, W. P.; Keller, R. A. Molecular shot noise, burst size distribution, and single-molecule detection in fluid flow: Effects of multiple occupancy. *J. Phys. Chem. A* **1998**, *102*, 6089−6094.
(51) Vukojević, V.; Pramanik, A.; Yakovleva, T.; Rigler, R.; Terenius, L.; Bakalkin, G. Study of molecular events in cells by fluorescence correlation spectroscopy. *Cell. Mol. Life Sci.* **2005**, *62*, 535−550.
(52) Krichevsky, O.; Bonnet, G. Fluorescence correlation spectroscopy: The technique and its applications. *Rep. Prog. Phys.* **2002**, *65*, 251−297.
(53) Enderlein, J.; Gregor, I.; Patra, D.; Fitter, J. Art and artifacts of fluorescence correlation spectroscopy. *Curr. Pharm. Biotechnol.* **2004**, *5*, 155−161.
(54) Hess, S. T.; Webb, W. W. Focal volume optics and experimental artifacts in confocal fluorescence correlation spectroscopy. *Biophys. J.* **2002**, *83*, 2300−2317.
(55) Eggeling, C.; Fries, J. R.; Brand, L.; Günther, R.; Seidel, C. A. M. Monitoring conformational dynamics of a single molecule by selective fluorescence spectroscopy. *Proc. Natl. Acad. Sci. U.S.A.* **1998**, *95*, 1556−1561.
(56) Culbertson, C. T.; Jacobson, S. C.; Ramsey, J. M. Diffusion coefficient measurements in microfluidic devices. *Talanta* **2002**, *56*, 365−373.
(57) Dertinger, T.; Pacheco, V.; von der Hocht, I.; Hartmann, R.; Gregor, I.; Enderlein, J. Two-focus fluorescence correlation spectroscopy: A new tool for accurate and absolute diffusion measurements. *ChemPhysChem* **2007**, *8*, 433−443.
(58) Tjernberg, L. O.; Pramanik, A.; Björling, S.; Thyberg, P.; Thyberg, J.; Nordstedt, C.; Berndt, K. D.; Terenius, L.; Rigler, R. Amyloid β-peptide polymerization studied using fluorescence correlation spectroscopy. *Chem. Biol.* **1999**, *6*, 53−62.
(59) Starchev, K.; Zhang, J.; Buffle, J. Applications of fluorescence correlation spectroscopy—Particle size effect. *J. Colloid Interface Sci.* **1998**, *203*, 189−196.
(60) Huang, B.; Perroud, T. D.; Zare, R. N. Photon counting histogram: One-photon excitation. *ChemPhysChem* **2004**, *5*, 1523−1531.
(61) Lappalainen, K.; Miettinen, R.; Kellokoski, J.; Jääskeläinen, I.; Syrjänen, S. Intracellular distribution of oligonucleotides delivered by cationic liposomes: Light and electron microscopic study. *J. Histochem. Cytochem.* **1997**, *45*, 265−274.
(62) Horn, E. F. Y.; Verkman, A. S. Analysis of coupled bimolecular reaction kinetics and diffusion by two-color fluorescence correlation spectroscopy: Enhanced resolution of kinetics by resonance energy transfer. *Biophys. J.* **2002**, *83*, 533−546.
(63) Barenholz, Y. Liposome application: Problems and prospects. *Curr. Opin. Colloid Interface Sci.* **2001**, *6*, 66−77.
(64) Zuidam, N. J.; Barenholz, Y. Electrostatic and structural properties of complexes involving plasmid DNA and cationic lipids commonly used for gene delivery? *Biochim. Biophys. Acta* **1998**, *1368*, 115−128.
(65) Ross, P. C.; Hui, S. W. Lipoplex size is a major determinant of in vitro lipofection efficiency. *Gene Ther.* **1999**, *6*, 651−659.
(66) Foquet, M.; Korlach, J.; Zipfel, W. R.; Webb, W. W.; Craighead, H. G. Focal volume confinement by submicrometer-sized fluidic channels. *Anal. Chem.* **2004**, *76*, 1618−1626.
(67) Kastrup, L.; Blom, H.; Eggeling, C.; Hell, S. W. Fluorescence fluctuation spectroscopy in subdiffraction focal volumes. *Phys. Rev. Lett.* **2005**, *94*, 178104.
(68) Rigneault, H.; Capoulade, J.; Dintinger, J.; Wenger, J.; Bonod, N.; Popov, E.; Ebbesen, T. W.; Lenne, P. F. Enhancement of single-molecule fluorescence detection in subwavelength apertures. *Phys. Rev. Lett.* **2005**, *95*, 117401.

BM700486Q